Energy states of quantum spin chain systems with p-adic coupling

Christopher Turchik Jagoe

April 2018

Advisor: Steven Gubser

Department of Physics

Princeton University

A senior thesis presented to the faculty of Princeton University in partial fulfillment of the degree of Bachelor of Arts.

Abstract

The correspondence between Anti-de Sitter space and conformal field theories has advanced our understanding of the connection between the fields of general relativity and quantum mechanics. It is possible to construct a discrete analog to AdS/CFT in which the AdS space is replaced by the p-adic Bruhat-Tits tree and Euclidean boundary by the p-adic numbers $\mathbb{Q}_p$. This thesis will investigate the quantum mechanical side of the duality through a treatment of spin-chain systems with p-adic coupling. First, an overview of the simpler Heisenberg ferromagnet is presented in order to develop the tools needed to analyze the more complex p-adic system. Then, a numeric calculation of the ground state for finite systems identifies regimes where single magnons dominate. Under these conditions, the thermodynamic limit is discussed and the specific heat and average energy are calculated. Like in the Heisenberg magnet, the specific heat increases as a power of the temperature, but the exact exponent depends on the strength of the p-adic, non-local interaction.

This paper represents my own work in accordance with University regulations.

Acknowledgements

I would like to thank my advisor, Steven Gubser, for his patience and support throughout my struggles with this thesis. When I came to your office in September knowing only the basics of quantum mechanics and even less about the specific topics that interested you, you kindly brought me up to speed. Your attention to detail, clear explanations, and ingenious solutions to difficult problems are qualities of a mentor I admire and wish to emulate.

I would also like to thank the graduate students, especially Christian Jepsen, for helping me to understand the topics we discussed in the research group. Your notes and comments allowed me to develop an intuition and familiarity with these abstract concepts.

I am indebted to the physics professors who have taught me and shaped my interests throughout my four years at Princeton. From freshman classes with Suzanne Staggs and Peter Meyers to advanced lab with Norm Jarosik, the faculty has been invaluable to my development as a student and scholar. A particular thanks is owed to Lyman Page and my second reader Herman Verlinde, for advising me through my two junior papers. You taught me how to approach a topic, formulate a research question, and professionally present my results.

To my fellow physics majors Paige, Jacob, Taylor, Charlie, Raheem, Nabai, and George, thank you for the hilarious entertainment that kept us sane through long hours of problem sets. Physics movie night and lunches at Tower always make me laugh. Thanks also to Easton, Jeffrey, Alex, and Matt for being great roommates and supportive friends. You guys have been my second family at school; may the quest for love soon be fulfilled.

Natalie, thank you for your constant love and support for the past year and a half. Walking the Camino, going to church, and translating the Bible with you has helped me to know God better. I am excited to continue this journey and "it has been a pleasure getting to know you."

I would like to dedicate this thesis to my high school physics teacher, Greg Devine. At Delbarton, you took my naïve enthusiasm for the subject and gave it discipline, a trellis on which the vine of academic zeal could grow. Your funny and idiosyncratic lectures, combined with serious advice on how to be better students and men, have motivated me to be a teacher, and I hope to be half as inspiring as you were for me and my classmates.

Finally, thank you to my parents and siblings for everything else. Ever since I started reading the *Oxford Children's Book of Science*, you have nurtured my love of learning. Through your countless sacrifices of time, money, and attention, you have shaped the person who I am and who I aspire to be.

Contents

Table of Figures

Chapter 1

Introduction and Motivation

Two broad fields underpin almost all of modern physics: quantum field theory (QFT) and general relativity (GR). The former describes the strong, weak, and electromagnetic forces; the latter provides a theory of gravity. Though physicists have experimentally confirmed almost every prediction that these theories make, the two are incompatible—they cannot both be true. The disagreement becomes pronounced when objects of study are either very small or have very high energy. For these regimes, a unified theory is sought, one which unites QFT and GR at a fundamental level. String theory currently stands out as the proposal with the most promise for the elusive theory of everything.

The basic premise of string theory is the existence of tiny vibrating strings that replace point particles like quarks and electrons. These strings are not immediately obvious because they are very small and exist in higher dimensions, which physicists claim are compactified, or rolled up tightly on themselves. With this outlook, not only are physical particles made of strings, but so too are force carriers, like the photon and the hypothetical graviton, which mediates gravity. String theory predicts the existence of a massless spin-2 particle; previous results have demonstrated that *any* spin-2 massless particle is consistent with the Einstein field equations and thus can be identified with the graviton [1]. The graviton is an example of a closed string, like a loop; the particles of quantum field theory are open strings, whose ends are fastened to higher dimensional analogues of strings called branes. Although it requires extra dimensions and makes many claims which are not experimentally proven, string theory thus comprises a framework to unify these drastically different forces of nature.

Even within string theory, variants and subvariants, with contrasting numbers of dimensions and

fundamental particles, take research into disparate directions. Currently, one of the most popular and fruitful areas of study is the AdS/CFT correspondence, which proposes a duality between anti-de Sitter space (AdS), a particular geometry of space-time, and conformal field theory (CFT), a set of quantum theories that possess a special type of symmetry. Rather than treating gravity, electromagnetism, etc., as different limits of the same theory, the AdS/CFT duality claims that two separate theories describe the same physical reality. Juan Maldacena published the seminal paper in 1997[2]. Supporting foundational work came a year later with papers by Gubser, Klebanov, and Polyakov [3] and by Witten [4], making Maldacena's conjecture more precise. In particular, Gubser et. al. linked the five-dimensional AdS_5 geometry with $\mathcal{N} = 4$ supersymmetric Yang-Mills theory, a gauge theory similar to quantum chromodynamics.

In general, anti-de Sitter space is a solution to Einstein's equations of general relativity with no matter field and constant negative curvature. A conformal field theory is a quantum field theory that is invariant under conformal, or locally angle-preserving transformations. The correspondence states that a CFT whose spacetime is the boundary of the AdS space is equivalent to the gravitational theory in the interior of that space. This interior is often called the "bulk" to distinguish from the quantum mechanical "boundary." Because it exists on the boundary, the CFT in n dimensions corresponds to AdS space in $n + 1$ dimensions. The correspondence posits the existence of a "holographic dictionary" for translating calculations in one theory to calculations in the other. The dictionary relates correlation functions of quantum operators to the action of a particle traveling in the bulk. For instance, for AdS_2/CFT_1, we have

$$\langle A(t_1)A^\dagger(t_2)\rangle = e^{-S} \approx \exp\big(\frac{i}{\hbar}m\int_1^2 ds\big). \tag{1.1}$$

The term on the left measures the overlap between the quantum vacuum state acted on by operator A at t_1 and the same vacuum state acted on at t_2. In the exponential, S is the action for a particle near the boundary, proportional to the path length of its trajectory. The two theories ought to be qualitatively identical, so that if some interaction would occur in the quantum theory with 30% probability, then the corresponding interaction in the gravitational world would also have 30% probability[5]. Such a duality is useful because intractable problems in one theory may be transformed and more easily worked out in the other. Though not yet formally proven, the increasing number of connections stands heavily in the favor of this correspondence.

This thesis studies a discretized version of a one-dimensional CFT, corresponding to two-dimensional AdS. Replacing the continuous interior geometry with a discrete lattice echoes a development in

string theory, where a regular graph similarly replaces a continuous manifold that describes how strings are embedded into spacetime. This graph is known as the Bruhat-Tits tree (Fig. 2.1) or the Bethe lattice with coordination number $p+1$, a cycle-free graph where each vertex has $p+1$ neighbors. The geometry of this tree is analogous to the group structure of AdS_2, which is the quotient group $SL(2,\mathbb{R})/U(1)$. Recall that $SL(2,\mathbb{R})$ is the special linear group, the set of 2×2 matrices with real entries and determinant 1, while $U(1)$ is the circle group, comprising all complex numbers with magnitude 1. The boundary of the tree also has a special structure, consisting of the field of p-adic numbers $\mathbb{Q}_p$ together with a "point at infinity," comprising the projective group $P^1(\mathbb{Q}_p)$. A more comprehensive overview of the p-adic numbers and the Bruhat-Tits tree will be given in Chapter 2. In general, however, the graph behaves like a discrete version of two-dimensional AdS space, while its boundary is the field $\mathbb{Q}_p$.

This thesis will focus on the conformal field theory side of the correspondence, with an analysis of spin chain systems whose interactions are governed by the p-adic norm. (For an account of the development gravitational equations of motion in the bulk, see Gubser [6] and Gift [7].) The quantum mechanical system consists of L spin-$\frac{1}{2}$ particles which interact with each other through various components of the spin operator $\vec{S}$. This setup can be viewed as a variation on the standard theory of magnetism with non-local interactions. Chapter 2 provides a more detailed introduction to the mathematics of the p-adic numbers, including properties of the Bruhat-Tits tree and p-adic integration. Chapter 3 begins with the quantum mechanical treatment of spin waves, contrasting the p-adic CFT with the standard Heisenberg model of magnetism. It proceeds to investigate the ground states and energy levels of spin chain systems over $\mathbb{Q}_p$. In Chapter 4, the thermodynamic properties of the system are discussed, including a calculation of average energy, specific heat, and magnetization. Appendix A contains the Mathematica and MATLAB code used to diagonalize the Hamiltonian, calculate the specific heat, and generate some figures.

There are two main results of this thesis. The first is evidence towards an assumption that, for large systems, low-energy, non-interacting magnons are the primary excitations away from an ordered ground state. Unlike in a traditional magnet, the spins in this p-adic system interact with many other spins instead of just their nearest neighbors, but changing this coupling does not cause complete disorder. As the number of sites grow large, thermodynamic properties can be calculated, relying on the fact that low energy states are the most prominent and eliminating dependence of the partition function on the exact energy levels. The second result is the discovery of power-law behavior for energy and specific heat at low temperatures. An equivalent of the famous Bloch three-halves law is developed for this system. Here, the exponent that governs scaling of these quantities

depends on the strength of non-local interactions in the system. With these properties in mind, more complicated systems can be studied, with the potential development of a discrete holographic dictionary, as discussed above.

Chapter 2

Mathematical Background

2.1 p-adic numbers

The real numbers $\mathbb{R}$ can be defined as equivalence classes of Cauchy sequences of rational numbers $\mathbb{Q}$. Let $\{a_n\}$ be a sequence of rational numbers and define $S_n \equiv \sum_{i=0}^{n} a_i$. A sequence is Cauchy if, for any $\varepsilon > 0$, there exists an integer N such that $m, n \geq N$ implies $|S_m - S_n| < \varepsilon$. Two Cauchy sequences are equivalent if the distance between them tends to zero. Under this equivalence relation, the real numbers $\mathbb{R}$ is just the set of all possible convergent series. It can be shown that this definition encapsulates all the usual properties of an ordered field. Notice, however, that the definition depended on the absolute value $|\cdot|$, the familiar notion of distance. If another norm is used, the rationals may be extended into a different field.

Let x be a rational number and express it as $x = \frac{p^a r}{s}$ where p is prime, and r, s are integers which are not divisible by p. Define the order of a p-adic number as $\text{ord}(x)_p = a$, the power to which the base prime is raised.Then the p-adic norm is

$$|x|_p = p^{-a}. \tag{2.1}$$

For instance, let $x = \frac{140}{297} = 2^2 \cdot 3^{-3} \cdot 5 \cdot 7 \cdot 11^{-1}$. Then $|x|_2 = 2^{-2}$, $|x|_3 = 3^3$, and $|x|_9 = 9^{-0}$. It can be shown that this operation has the usual properties of a norm: scalability, positive definiteness, and subadditivity. It differs from the norm on $\mathbb{R}$ because it is ultrametric, i.e., for any numbers y, z,

$$|y + z|_p \leq \max\{|y|_p, |z|_p\}. \tag{2.2}$$

Ultrametricity implies that the Archimedean property does not hold, which states that if $0 < |y| < |z|$, then for some integer n, $|ny| > |z|$. With the ultrametric p-adic norm, however, $|ny|_p < |y|_p < |z|_p$.

why is this important

A general p-adic number can be expanded as a formal power series

$$x = p^a \sum_{m=0}^{\infty} c_m p^m \tag{2.3}$$

where c_m are the digits in the base p expansion, chosen from the set $\{0, 1, \ldots, p-1\}$. The order a is the largest integer such that the first digit c_0 is not zero. Because the p-adic norm assigns lower values to larger powers of p, this power series gives a number that terminates on the right and may extend infinitely to the left. For example, if $p = 5$, then

$$-\frac{1}{24} = \frac{1}{1-25} = 1 + 5^2 + 5^4 + \cdots = \ldots 0101_5. \tag{2.4}$$

2.2 Bruhat-Tits tree

With this formal expansion in mind, the p-adic numbers can be represented graphically on the Bruhat-Tits tree, Fig. 2.1. Consider a $p+1$-regular tree (a graph such that there are no closed loops and every vertex has $p+1$ neighbors). Choose an arbitrary oriented path through the tree, called the trunk, and label one end as 0 and the other ∞. The trunk in 2.1 is highlighted in red. Every point in $\mathbb{Q}_p$ then may be considered as the termination point of some unique path that starts on the trunk at ∞. Several observations make navigation on this tree more intuitive. Let some point on the trunk denote the p^0 level. Successive vertices "above" and "below" this point will correspond to positive and negative powers of p, as labeled. For any particular path, the first point of departure from the trunk indicates the first non-zero power of p in an expansion like (2.4), counting from the most significant power (rightmost digit in the expansion). If the branch-off occurs at p^v, then the number at the termination of the path will have magnitude p^{-v}. For example, numbers whose paths branch off at non-negative powers of p will have a magnitude of no more than 1, so they are the p-adic integers $\mathbb{Z}_p$. The Bruhat-Tits tree conveniently groups this set together. Additionally, the choice of vertex at each level corresponds to the digit in the p-adic expansion of the number. With the 2-adic example here, each next step can add $0 \times p^n$ or $1 \times p^n$, but in general, there is a p-fold choice at each vertex.

Let z be a p-adic number and z_0 a depth. The coordinate pair (z_0, z) is used to (non-uniquely)

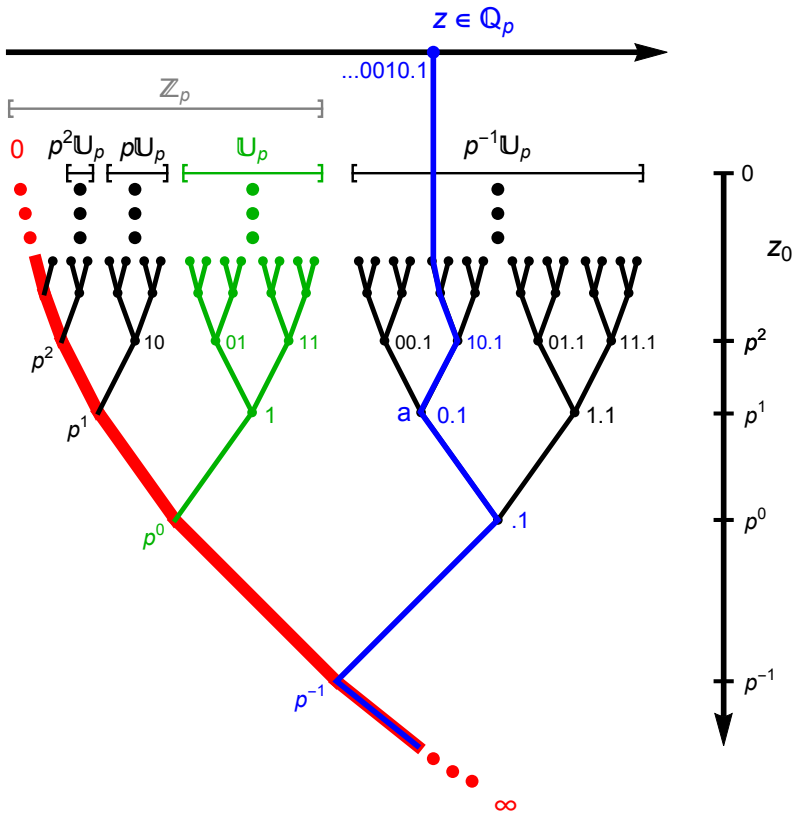

Figure 2.1: The Bruhat-Tits tree for $p = 2$. The trunk, leading to 0, is shown in red. The blue path leads to the specific 2-adic number $\ldots 0010.1$. The green section highlights paths leading to elements of $\mathbb{U}_p$, the p-adic units.

specify a vertex a, which lives at depth z_0 and from which the number z is reachable. Clearly, many different values of z can describe the same vertex if their paths lie in the same sub-branch of the tree; therefore, we identify the points (z_0, z) and $(z_0, \tilde{z},)$ if $|\tilde{z} - z|_p \leq |z_0|_p$. Looking at the vertices of the tree with these coordinates hints at a correspondence with continuous, Archimedean anti-de Sitter space, which has similar properties.

2.3 p-adic integration

The p-adic numbers admit all the usual operations of a field. They also admit integration of functions. This section will provide a brief introduction to p-adic integration as it will be applied later on.

There are three fundamental identities from which all p-adic integrals descend.

$$\int_{\mathbb{Z}_p} dx = 1, \tag{2.5}$$

where $\mathbb{Z}_p = \{x \in \mathbb{Q}_p : |x|_p \leq 1\}$. $\mathbb{Z}_p$, the p-adic integers, is a fundamental ring [8]. This set is

similar to the interval $[-1,1] \subset \mathbb{R}$, the numbers with absolute value less than 1. The integral is scale invariant: for any number b,

$$\int_{\mathbb{Z}_p+b} dx = 1. \tag{2.6}$$

The last identity is related to scaling:

$$\int_{a\mathbb{Z}_p} dx = |a|_p. \tag{2.7}$$

Notice that scaling the integers produces a subset of the integers: $p\mathbb{Z}_p \subset \mathbb{Z}_p$. Many of the functions we will want to integrate map the p-adic integers $\mathbb{Z}_p$ into the complex numbers $\mathbb{C}$ and have their image equal to a countable subset, say $C \subset \mathbb{C}$. If we want to calculate the integral $\int_A f(x)dx$ for a measurable set A, first partition the domain into level sets

$$A_f(c) = \{x \in A | f(x) = c\}. \tag{2.8}$$

Then we can compute the integral as [9]

$$\int_A f(x)dx = \sum_{c\in C} \int_{A_f(c)} f(x)dx = \sum_{c\in C} c \cdot \mathrm{Vol}(A_f(c)). \tag{2.9}$$

Let us apply this technique with an example, the integral

$$\int_{|x|_p>1} \frac{1}{|x|^s} dx. \tag{2.10}$$

First, define the set of p-adic units $\mathbb{U}_p \equiv \mathbb{Z}_p \setminus p\mathbb{Z}_p$. The level sets in this case are scaled copies of $\mathbb{U}_p$, since $|x|_p^s = p^{-ns}$ when $x \in p^n\mathbb{U}_p$. Now let's compute the volume of the level sets. By the scaling property, $\int_{p\mathbb{Z}_p} dx = \frac{1}{p}$, so

$$\mathrm{Vol}(\mathbb{U}_p) = \int_{\mathbb{U}_p} dx = \int_{\mathbb{Z}_p} dx - \int_{p\mathbb{Z}_p} dx = 1 - \frac{1}{p}. \tag{2.11}$$

Use the scaling property again to obtain $\mathrm{Vol}(p^n\mathbb{U}_p) = |p^n|_p(1-\frac{1}{p}) = p^{-n}(1-\frac{1}{p})$. We check that the domain of integration $|x|_p > 1$ can be written as the union of these sets, negatively indexed:

$$\bigcup_{n=-\infty}^{-1} p^n\mathbb{U}_p = \bigcup_{n=-\infty}^{-1} \left(p^n\mathbb{Z}_p \setminus p^{n+1}\mathbb{Z}_p\right) = p^{-1}\mathbb{Z}_p \setminus p\mathbb{Z}_p \ \cup \ p^{-2}\mathbb{Z}_p \setminus p^{-1}\mathbb{Z}_p \ \cup \cdots = \mathbb{Q}_p \setminus \mathbb{Z}_p. \tag{2.12}$$

The partition is a telescoping union that results in our desired set. Then the integral reduces to a

geometric series

$$\int_{|x|_p>1} \frac{dx}{|x|_p^s} = \sum_{n=-\infty}^{-1} \frac{1}{p^{-ns}} p^{-n} \left(1 - \frac{1}{p}\right). \tag{2.13}$$

Expand the first few terms of the series

$$\begin{aligned}
\sum_{n=-\infty}^{-1} \frac{1}{p^{-ns}} p^{-n} \left(1 - \frac{1}{p}\right) &= \frac{1}{p^s} p \left(1 - \frac{1}{p}\right) + \frac{1}{p^{2s}} p^2 \left(1 - \frac{1}{p}\right) + \frac{1}{p^{3s}} p^3 \left(1 - \frac{1}{p}\right) + \cdots && (2.14)\\
&= \left(\frac{1}{p^{s-1}} + \frac{1}{p^{2(s-1)}} + \frac{1}{p^{3(s-1)}} + \cdots\right) \left(1 - \frac{1}{p}\right) && (2.15)\\
&= \left(\frac{1}{p^{s-1} - 1}\right) \left(1 - \frac{1}{p}\right) && (2.16)\\
&= \frac{p-1}{p^s - p}. && (2.17)
\end{aligned}$$

This simple example provides the technique for tackling more complicated examples that will arise later.

Chapter 3

Energy Levels

3.1 Spin chain systems

In this thesis, the basic quantum system under consideration is a chain of L interacting spin-$\frac{1}{2}$ particles. The most general Hamiltonian is

$$H \equiv \frac{1}{2} \sum_{m_1,m_2} J_{m_1,m_2} \mathfrak{h}_{m_1 m_2} \tag{3.1}$$

where m_1 and m_2 denote particular spins and run from 0 to $L-1$. The coefficients J_{m_1,m_2} indicate the strength of the interaction between the indicated spins. At this point, the only restrictions on the coefficients are translation invariance and symmetry:

$$J_{m_1,m_2} = J_{m_2,m_1} = J_{m_1-m_2}. \tag{3.2}$$

The $\mathfrak{h}_{m_1 m_2}$ term is shorthand notation for a range of coupling types. As shown in [10], we have, in full,

$$\mathfrak{h}_{m_1 m_2} \equiv 2\vec{S}_{m_1} \cdot \vec{S}_{m_2} + 2(\alpha - 1) S^z_{m_1} S^z_{m_2} \tag{3.3a}$$

$$= S^+_{m_1} S^-_{m_2} + S^-_{m_1} S^+_{m_2} + 2\alpha S^z_{m_1} S^z_{m_2}. \tag{3.3b}$$

$\vec{S}$ are spin vectors for each site, shorthand for the vector of operators (S_x, S_y, S_z). Each of these component operators can be represented by the Pauli matrices. The ladder operators $S^{\pm} \equiv S_x \pm i S_y$ are the standard combinations of the cartesian components of the spin; they raise or lower the spin

quantum number of a state. The adjustable parameter α is provided for generality. For $\alpha \gg 1$, the z coupling dominates and the system is approximately Ising. $\alpha = 1$ corresponds to the isotropic or "spin-dot" Heisenberg model, named since the spins interact through the dot product of their vectors. $\alpha = 0$ is a an XY-coupling, also called a "plus-minus" coupling. Other values define the general XXZ Heisenberg model which can be solved and approximated by various methods, including the Bethe ansatz. Often, a magnetic field is applied to these spin systems in a fixed direction. The Hamiltonian receives an additional term

$$H \equiv \frac{1}{2} \sum_{m_1,m_2} J_{m_1,m_2} \mathfrak{h}_{m_1 m_2} - b \sum_{m_1} S^z_{m_1} \tag{3.4}$$

which eliminates the degeneracy of some states. Before, the two states with all spins pointing in the same direction had the same energy. Now, the system has a preferred direction, and these two states have different energies. The magnetic field will be useful later on in identifying the ground states of systems with different couplings.

3.2 Going deeper

Treatment of the model depends uses two operators which commute with the Hamiltonian and with each other. The first is the total z spin of the system:

$$S^z_{\text{total}} = \sum_m S^z_m. \tag{3.5}$$

The individual S^z_m do not commute with H due to the presence of S^x and S^y terms. The total spin does, however:

$$[S^z_{\text{total}}, H] = \frac{1}{2} \sum_{ijk} J_{ij} \left[S^z_k, S^x_i S^x_j + S^y_i S^y_j + S^z_i S^z_j \right] \tag{3.6a}$$

$$= \frac{1}{2} \sum_{ijk} J_{ij} \left(S^x_i \left[S^z_k, S^x_j \right] + \left[S^z_k, S^x_i \right] S^x_j + S^y_i \left[S^z_k, S^y_j \right] + \left[S^z_k, S^y_i \right] S^y_j + 0 \right) \tag{3.6b}$$

$$= \frac{1}{2} \sum_{ijk} J_{ij} \left(S^x_i \delta_{kj} S^y_j + \delta_{ki} i S^y_i S^x_j + S^y_i \delta_{kj} (-i) S^x_j + \delta_{ki} (-i) S^x_i S^y_j + 0 \right) = 0. \tag{3.6c}$$

The same result holds for any component of total spin, which means we can find simultaneous eigenstates of H, $\vec{S}_{\text{total}} \cdot \vec{S}_{\text{total}}$, and S^z_{total} [11]. The second is the translation operator U, defined to

map the m-th spin's vector space to the space of the $(m-1)$-th:

$$U\vec{S}_m U^{-1} = \vec{S}_{m-1}. \tag{3.7}$$

We assume cyclic boundary conditions, i.e., $U^L = \mathbf{1}$. The eigenvalues of U are therefore the L-th roots of unity, $e^{2k\pi i/L}$, with $k \in \mathbb{Z}$. Because $k \to k+L$ leaves the phase unchanged, k, along with the may be considered to take values in the ring $\mathbb{Z}/L\mathbb{Z}$. For convenience, we can make the definition

$$\chi(\xi) = e^{2\pi i\xi/L}. \tag{3.8}$$

This translation operator commutes with the Hamiltonian, so Noether's theorem requires the existence of a conserved quantity, something like momentum. What particle possesses this momentum will be explained later on, but this link is enough motivation to look for the eigenstates of U in the same way as the plane-wave eigenstates for momentum in a continuous system. These states will be simultaneous eigenstates of H and S^z_{total} as well. We will describe the system using the S^z basis. For each site let

$$\chi_+ = \begin{pmatrix}1\\0\end{pmatrix} = \left|S^z_m = +\tfrac{1}{2}\right\rangle = |\uparrow\rangle = |0\rangle \tag{3.9a}$$

$$\chi_- = \begin{pmatrix}0\\1\end{pmatrix} = \left|S^z_m = -\tfrac{1}{2}\right\rangle = |\downarrow\rangle = |1\rangle \tag{3.9b}$$

denote the two eigenstates of S^z_m. These vectors span the two-dimensional Hilbert space of each spin. The Hilbert space of the whole system has dimension 2^L and is spanned by the tensor products of the 2^L combinations of the $|\uparrow\rangle$ and $|\downarrow\rangle$ vectors for each site. One important vector, representing the state with all spins up, will be denoted

$$|\Omega\rangle \equiv \underbrace{\begin{pmatrix}1\\0\end{pmatrix} \otimes \begin{pmatrix}1\\0\end{pmatrix} \otimes \cdots \otimes \begin{pmatrix}1\\0\end{pmatrix}}_{L \text{ times}} = |\uparrow\uparrow \ldots \uparrow\rangle \ . \tag{3.10}$$

Let L_- be the number of down spins, so $S^z_{total} = \frac{L}{2} - L_-$. Clearly $|\Omega\rangle$ is the unique state with $L_- = 0$, and $U|\Omega\rangle = |\Omega\rangle$. The energy for this state is also easy to find. The magnetic field term gives a contribution of $-\frac{1}{2}bL$. Because we assumed translation invariance, let h denote the distance

between two sites. Then

$$-\frac{1}{2}\sum_{m_1,m_2} J_{m_1,m_2}\left(S^+_{m_1}S^-_{m_2}+S^-_{m_1}S^+_{m_2}\right)|\Omega\rangle = -\frac{1}{2}\sum_{i=0}^{L-1}\sum_{h=0}^{L-1} J_h(S^+_i S^-_{i+h}+S^-_i S^+_{i+h})|\Omega\rangle = -\frac{1}{2}LJ_0|\Omega\rangle \tag{3.11}$$

since the $S^{\pm}$ terms are zero except when S^-_i first lowers spin i and then S^+_i raises it again. Otherwise S^+ acting on a spin that is already up produces zero. The S^z terms give a more straightforward result:

$$-\frac{1}{2}\sum_{m_1,m_2} J_{m_1,m_2}\left(2\alpha S^z_{m_1}S^z_{m_2}\right)|\Omega\rangle = -\alpha\sum_{i=0}^{L-1}\sum_{h=0}^{L-1} J_h S^z_i S^z_{i+h}|\Omega\rangle = -\frac{\alpha L}{4}\sum_{h=0}^{L-1} J_h|\Omega\rangle \tag{3.12}$$

It is now useful to define Fourier transforms and inverse transforms in the following form:

$$f_n = \frac{1}{\sqrt{L}}\sum_{k=0}^{L-1}\chi(kn)\tilde{f}_\kappa \qquad\qquad \tilde{f}_\kappa = \frac{1}{\sqrt{L}}\sum_{n=0}^{L-1}\chi(-kn)f_n\,. \tag{3.13}$$

Therefore, we write the Schrödinger equation for $|\Omega\rangle$ as $H|\Omega\rangle = E_\Omega|\Omega\rangle$ where

$$E_\Omega = -L\left(\frac{\alpha}{4}\sqrt{L}\tilde{J}_0+\frac{1}{2}J_0+\frac{1}{2}b\right). \tag{3.14}$$

After the simple ferromagnetic state, the next-easiest states to organize are those for which $L_- = 1$. This set is an L-dimensional subspace of the full 2^L dimensional Hilbert space and is spanned by the L different states $S^-_m|\Omega\rangle$. Rather than using the product basis, which is utilized later on in Section 3.3, we can use orthonormal eigenvectors of U:

$$|\kappa\rangle \equiv \frac{1}{\sqrt{L}}\sum_{n=0}^{L-1}\chi(\kappa n)S^-_n|\Omega\rangle\,. \tag{3.15}$$

It is easy to see that $U|\kappa\rangle = \chi(\kappa)|\kappa\rangle$, so we say that state $|\kappa\rangle$ has momentum κ. It is called the one-magnon state. Because U, S^z_total and H all commute with each other, $|\kappa\rangle$ must be a simultaneous eigenstate of H, and indeed, $H|\kappa\rangle = E_\kappa|\kappa\rangle$ with

$$E_1(\kappa) - E_\Omega = \alpha\sqrt{L}\tilde{J}_0 - \sqrt{L}\tilde{J}_\kappa - (\alpha-1)J_0 - \frac{1}{2}b\,. \tag{3.16}$$

Recall that $\tilde{J}_0$ and $\tilde{J}_\kappa$ are sums of the coupling coefficients, and these sums include J_0. In (3.16), the third term combines with the first two to eliminate the dependence of J_0 on $E_\kappa - E_\Omega$. Essentially, the energy gap between the two states does not depend on the self-coupling term J_0, since J_0 multiplies

$\mathfrak{h}_{mm}$, which is proportional to the identity matrix.

3.3 What is a magnon?

A magnon is a quantized spin wave. We call the state $|\kappa\rangle$ the one-magnon state because it is the average of states with one spin flipped down, where the flipped spin "advances" as we go through the sum. For instance, with $L = 4$ and $\kappa = 1$, we write out

$$|\kappa = 1\rangle = \frac{1}{\sqrt{L}}\left[|\downarrow\uparrow\uparrow\uparrow\rangle + e^{\pi i/2}\,|\uparrow\downarrow\uparrow\uparrow\rangle + e^{\pi i}\,|\uparrow\uparrow\downarrow\uparrow\rangle + e^{3\pi i/2}\,|\uparrow\uparrow\uparrow\downarrow\rangle\right]. \tag{3.17}$$

The coefficient of each successive term differs by a phase factor of $e^{\pi i/2}$, hinting at a wavelike property. To illustrate this phenomenon, we will make use of a common and simple coupling pattern: nearest neighbor coupling. Each spin will be allowed to interact with the spins on either side of it. This assumption is a physical one; the Heisenberg model of magnetism works in this way. Take the Hamiltonian of (3.1) and impose

$$J_h^{NN} = J_*\left(\delta_{h+1} + \delta_{h-1} - 2\delta_h\right), \tag{3.18}$$

where J_* is a constant. Along with taking $\alpha = 1$ and omitting the magnetic field ($b = 0$), the Hamiltonian simplifies to

$$H^{NN} = -2J_* \sum_{m=1}^{N} \vec{S}_m \cdot \vec{S}_{m+1}. \tag{3.19}$$

The ground state for this system is the ferromagnetic state $|\Omega\rangle$ with all spins aligned. When H^{NN} acts on this state, $\vec{S}_m \cdot \vec{S}_{m+1} = S^2 = \frac{1}{4}$, and the ground state energy is $U_0 = -\frac{1}{2}LJ_*$. One way to produce an excited state is to flip the spin at the i-th position. This change results in a new eigenstate which has an additional $2J_*$ of energy. However, if the $\pi/2$ rotation is shared among all the spins, so that each differs from the previous by an angle of $\pi/2L$ (see Fig.3.1), the increase in energy is much lower. The system still has a total z spin of $L - 1$, but each spin is still largely aligned with its neighbors. These elementary excitations of the spin chain have a wave-like form: the magnons. The amount by which the phase advances is the momentum κ, in analogy with a physical wave whose wavenumber is related to its physical momentum. Although this image treats the spins as classical vectors, the intuition is largely the same. It is possible, as shown below, to derive some properties of magnons by quantum mechanical arguments.

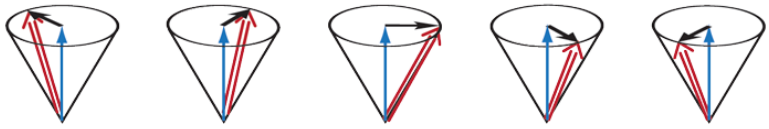

Figure 3.1

Rewrite the Hamiltonian in 3.19 in terms of the Pauli spin exchange operator $P_{m,m+1}$

$$H = -\frac{1}{2}J_* \sum_m (2P_{m,m+1} - 1). \tag{3.20}$$

This operator interchanges the spins at the indexed sites: $P|\uparrow\downarrow\rangle = \pm\,|\downarrow\uparrow\rangle$. Repeated application of the exchange operator returns the original wavefunction. Therefore $P^2 = \mathbf{1}$, leaving both $+1$ and -1 as possible eigenvalues for P. States that pick up a negative sign under exchanged are the fermions, while those that do not are the bosons. To show that the Hamiltonian of (3.20) is equivalent to (3.19) is accomplished by looking at their actions on a convenient choice of basis vectors. First, rewrite $\vec{S}_1 \cdot \vec{S}_2$ as $\frac{1}{2}\left(\left(\vec{S}_1 + \vec{S}_2\right)^2 - \vec{S}_1^2 - \vec{S}_2^2\right)$. The eigenvalue for any S^2 operator is $S(S+1)$. Then, note that for the three triplet states

$$\left.\begin{array}{lcl} |1,1\rangle & = & |\uparrow\uparrow\rangle \\ |1,0\rangle & = & \left(|\uparrow\downarrow\rangle + |\downarrow\uparrow\rangle\right)/\sqrt{2} \\ |1,-1\rangle & = & |\downarrow\downarrow\rangle \end{array}\right\} \quad s = 1 \quad \text{(triplet)} \tag{3.21}$$

the operators $2\vec{S}_1 \cdot \vec{S}_2$ and $\frac{1}{2}(2P - 1)$ are equal with eigenvalue $\frac{1}{2}$, while for the singlet state

$$\left.|0,0\rangle = \left(|\uparrow\downarrow\rangle - |\downarrow\uparrow\rangle\right)/\sqrt{2}\right\} \quad s = 0 \quad \text{(singlet)} \tag{3.22}$$

they have eigenvalue $-\frac{3}{2}$. The derivation can be further simplified by ignoring the constant contribution of the zero point energy $-\frac{1}{2}LJ_*$. Subtracting this off, the Hamiltonian 3.20 becomes

$$H = -J_* \sum_m (P_{m,m+1} - 1). \tag{3.23}$$

Our working basis for the $L_- = 1$ Hilbert space will be $|m\rangle$ which denotes the m-th spin flipped down and the others remaining up. A general wavefunction $|\psi\rangle$ can be decomposed into this basis

by inserting a complete set of states by

$$|\psi\rangle = \sum_m |m\rangle \langle m|\psi\rangle \,. \tag{3.24}$$

Then apply the Schrödinger equation and take the inner product with an arbitrary $\langle n|$ to obtain

$$-J_* \sum_i \sum_m \langle n|(P_{i,i+1} - 1)|m\rangle \langle m|\psi\rangle = \mathcal{E} \langle n|\psi\rangle \,, \tag{3.25}$$

where $\mathcal{E}$ is the eigenvalue, the energy of state $|\psi\rangle$. What is the action of the parity operator on these basis states? If $m \neq i, i+1$, then two parallel spins are exchanged, leaving the wavefunction unchanged, so $(P_{i,i+1} - 1)|m\rangle = 0$. If $m = i, i+1$, then the flipped spin at place m is transferred to the right or left, so

$$(P_{m,m+1} - 1)|m\rangle = |m+1\rangle - |m\rangle \tag{3.26}$$

$$(P_{m-1,m} - 1)|m\rangle = |m-1\rangle - |m\rangle \,. \tag{3.27}$$

We can substitute these relations into the Schrödinger equation, leading to

$$-J_* \sum_m \langle n| \left(|m+1\rangle - |m\rangle + |m-1\rangle\right) \langle m|\psi\rangle = \mathcal{E} \langle n|\psi\rangle \,, \tag{3.28}$$

where $\mathcal{E}$ is the eigenvalue, the energy of the state. Many of these inner products are zero because the basis states are orthonormal: $\langle m|n\rangle = \delta_{mn}$. After summation, (3.28) simplifies to

$$-J_* \left(\langle n-1|\psi\rangle + \langle n+1|\psi\rangle - 2\langle n|\psi\rangle\right) = \mathcal{E} \langle n|\psi\rangle \,. \tag{3.29}$$

Let the location of the nth spin be x_n and the spacing between spins be a. Then for an Ansatz, the following can be used:

$$\langle n|\psi\rangle \equiv C(x_n) \tag{3.30}$$

$$\langle n \pm 1|\psi\rangle \equiv C(x_n \pm a). \tag{3.31}$$

Here, $C(x_n)$ is a function of position which gives the coefficients for decomposing any state into this

basis. The Schrödinger equation becomes a difference equation

$$-\frac{\mathcal{E}}{J_*}C(x_n) = C(x_n - a) + C(x_n + a) - 2C(x_n) \tag{3.32}$$

which has a solution of the form

$$C(x_n) = \frac{1}{\sqrt{L}}e^{ikx_n}. \tag{3.33}$$

We have now identified the coefficients of $\langle n|\psi\rangle$, the projection of $|\psi\rangle$ onto the basis vectors. Notice that they are normalized and that the probability of finding a flipped spin at any particular site is the same, $|\langle n|\psi\rangle|^2 = 1/L$. Thinking semi-classically, two adjacent spins that participate in a spin wave mode with wavevector k have an angle between them equal to ka. If we insert the trial solution and use the identity $\cos x = \frac{1}{2}(e^{ix} + e^{-ix})$, we can simplify to find the energy of the spin wave in terms of the wavevector k:

$$\mathcal{E} = 2J_*(1 - \cos ka). \tag{3.34}$$

This relationship is called the dispersion relation. For states with a low momentum and a long wavelength compared to the spacing between the spins ($ka \ll 1$), the cosine term can be Taylor expanded to

$$\mathcal{E} \approx J_* k^2 a^2 + O(k^4 a^4). \tag{3.35}$$

As $L \to \infty$, this approximation becomes more realistic. This quadratic relationship distinguishes magnons from other quasiparticles, such as phonons, which have a linear dispersion relation. The solution also indicates a physical interpretation: if several solutions with closely spaced frequency components are added together, a wave packet can be formed with an effective mass of

$$m = \frac{1}{2J_* a^2}. \tag{3.36}$$

3.4 Calculations

Magnons are well-behaved and well-studied in the Heisenberg ferromagnetic model. In fact, for nearest-neighbor coupling, a sophisticated technique called the Bethe Ansatz can be used to calculate the eigenvalues and eigenstates explicitly, without treating magnons as perturbations around an ordered state. When we introduce all-to-all or all-to-many couplings, however, the system becomes more complicated. To return to the idea of the p-adic AdS/CFT correspondence, we introduce new

coupling patterns. The most important is the p-adic coupling

$$J_h^{p-\text{adic}} = J_* |h|_p^{-s-1}. \tag{3.37}$$

With this choice of coefficients, spins that are a small p-adic distance away interact strongly. Another

p-adic dispersion relation!

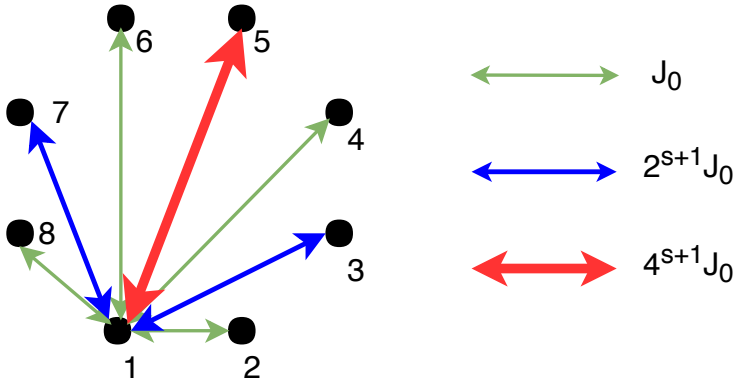

Figure 3.2: 2-adic coupling for $L = 8$ sites. As shown, spin 1 interacts most strongly with spin 5, which is farthest away from it by Euclidean measurement but closest p-adically. The coupling pattern is translation invariant, so spins 2 and 6 are as strongly coupled as spins 1 and 5, for example.

coupling is the sparse coupling, which interpolates between $J^{p\text{-adic}}$ and J^{NN}:

$$J_h^{\text{sparse}} = J_* \sum_m^{L-1} 2^{ns} \left(\delta_{h-2^n} + \delta_{h+2^n} - 2\delta_h\right) \tag{3.38}$$

When the magnetic field is non-zero, the totally ordered ferromagnetic state $|\Omega\rangle$ is no longer always the ground state. Certain combinations of magnetic field strength b and interaction strength J_*, along with the highly non-local couplings, conspire to induce different states of the system. For small numbers of sites, it is possible to explicitly compute the states and the energies.

more on the couplings, introduce monna map

We begin with $L = 4$ sites, which live in a Hilbert space of $2^L = 16$ dimensions. The matrices of interest are formed from vector products of the 2×2 Pauli matrices

$$\sigma_x = \begin{pmatrix} 0 & 1 \\ 1 & 0 \end{pmatrix} \qquad \sigma_y = \begin{pmatrix} 0 & -i \\ i & 0 \end{pmatrix} \qquad \sigma_z = \begin{pmatrix} 1 & 0 \\ 0 & -1 \end{pmatrix}. \tag{3.39}$$

By itself, the S^z operator is defined as $S_i^z = \sigma_z/2$. If it acted on, say, the second spin in this system. because it only acts on this spin, it is tensored together with the 2×2 identity matrices that operate

on the other spins. Thus, in this system, using the product basis, we define

$$S_2^z = I \otimes \frac{1}{2}\sigma_z \otimes I \otimes I \tag{3.40}$$

$$= \begin{pmatrix}
1 & 0 & 0 & 0 & 0 & 0 & 0 & 0 & 0 & 0 & 0 & 0 & 0 & 0 & 0 & 0 \\
0 & 1 & 0 & 0 & 0 & 0 & 0 & 0 & 0 & 0 & 0 & 0 & 0 & 0 & 0 & 0 \\
0 & 0 & 1 & 0 & 0 & 0 & 0 & 0 & 0 & 0 & 0 & 0 & 0 & 0 & 0 & 0 \\
0 & 0 & 0 & 1 & 0 & 0 & 0 & 0 & 0 & 0 & 0 & 0 & 0 & 0 & 0 & 0 \\
0 & 0 & 0 & 0 & -1 & 0 & 0 & 0 & 0 & 0 & 0 & 0 & 0 & 0 & 0 & 0 \\
0 & 0 & 0 & 0 & 0 & -1 & 0 & 0 & 0 & 0 & 0 & 0 & 0 & 0 & 0 & 0 \\
0 & 0 & 0 & 0 & 0 & 0 & -1 & 0 & 0 & 0 & 0 & 0 & 0 & 0 & 0 & 0 \\
0 & 0 & 0 & 0 & 0 & 0 & 0 & -1 & 0 & 0 & 0 & 0 & 0 & 0 & 0 & 0 \\
0 & 0 & 0 & 0 & 0 & 0 & 0 & 0 & 1 & 0 & 0 & 0 & 0 & 0 & 0 & 0 \\
0 & 0 & 0 & 0 & 0 & 0 & 0 & 0 & 0 & 1 & 0 & 0 & 0 & 0 & 0 & 0 \\
0 & 0 & 0 & 0 & 0 & 0 & 0 & 0 & 0 & 0 & 1 & 0 & 0 & 0 & 0 & 0 \\
0 & 0 & 0 & 0 & 0 & 0 & 0 & 0 & 0 & 0 & 0 & 1 & 0 & 0 & 0 & 0 \\
0 & 0 & 0 & 0 & 0 & 0 & 0 & 0 & 0 & 0 & 0 & 0 & -1 & 0 & 0 & 0 \\
0 & 0 & 0 & 0 & 0 & 0 & 0 & 0 & 0 & 0 & 0 & 0 & 0 & -1 & 0 & 0 \\
0 & 0 & 0 & 0 & 0 & 0 & 0 & 0 & 0 & 0 & 0 & 0 & 0 & 0 & -1 & 0 \\
0 & 0 & 0 & 0 & 0 & 0 & 0 & 0 & 0 & 0 & 0 & 0 & 0 & 0 & 0 & -1
\end{pmatrix}. \tag{3.41}$$

It is apparent that matrices in this system rapidly become unwieldy, so they will not be written. In the same manner, we can produce the Hamiltonian for the system, and diagonalize it. There are two variations that will be dealt with here: in the first, the spins interact through their dot product $\vec{S} \cdot \vec{S}$, which corresponds to $\alpha = 1$ in (3.1). The second uses $\alpha = 0$, for which only the $S^+_{m_1} S^-_{m_2} + S^-_{m_1} S^+_{m_2}$ terms contribute. This "plus-minus" coupling can be more easily experimentally realized, as indicated by the preliminary cold atom experiments of M. Schleier-Smith and Greg Benson. Plus-minus coupling actually also yields more interesting results. cite

For this setup, neighboring sites have a 2-adic distance and a Euclidean distance of 1. The cross-terms, pairing spin 1 to spin 3 and spin 2 to spin 4, have a 2-adic distance of $\frac{1}{2}$, so they will be given a weighting of 2^{s+1} relative to the nearest neighbor interactions. In the plots below, we set $J \equiv 2^{s+1}$ so that $\log_2 J = s + 1$. Varying J thus effectively changes the strength of the p-adic coupling. After diagonalization, we find that there are twelve unique eigenvalues, listed here with multiplicity in parentheses. They are 0 (3), $\pm 2b$, $-J \pm 2 \pm b$, $2J$, $J \pm b$ (2), $-J \pm \sqrt{8 + J^2}$. These

possible energies, normalized by $\sqrt{J}$, are plotted below for $b = 2.78$ in Figure 3.3. The red line is merely a guide for the eye to select a particular energy state.

when do you get pluses or minuses? when do the states depend on J?

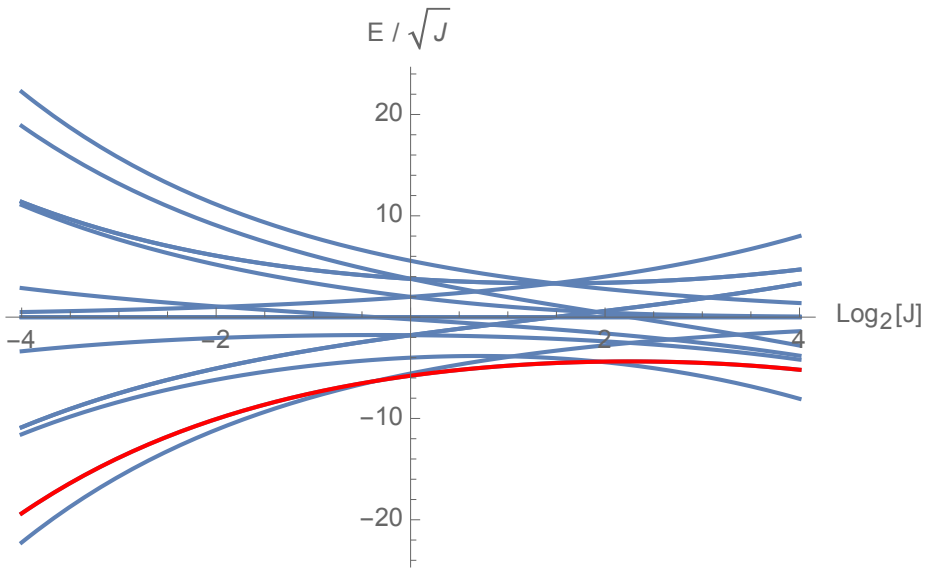

Figure 3.3: The energy levels of the $L = 4$ 2-adic system with plus-minus coupling. The magnetic field is set to $b = 3$ for this figure. The red line guides the eye to indicate that that particular level is the ground state for a small range near $\log_2 J = 0.5$.

After examining the energy levels for a range of b values, there are three levels that compete for the ground state. The first is the obvious ferromagnetic ground state $|\uparrow\uparrow\uparrow\uparrow\rangle$. This state has energy $-2b$, independent of the strength of the cross-coupling parameterized by J. It is the ground state when b is large and J is small. The second potential ground state is the zero-momentum magnon

why?

$$|k = 0\rangle = |\downarrow\uparrow\uparrow\uparrow\rangle + |\uparrow\downarrow\uparrow\uparrow\rangle + |\uparrow\uparrow\downarrow\uparrow\rangle + |\uparrow\uparrow\uparrow\downarrow\rangle \ . \tag{3.42}$$

This one dominates when J and b are closer in magnitude and has energy $-2 - b - J$. Finally, a complicated ground state wins when J is large or b is very small. It spans the two-magnon subspace and is equal to

$$|2 \text{ magnons}\rangle = |\downarrow\downarrow\uparrow\uparrow\rangle + |\downarrow\uparrow\uparrow\downarrow\rangle + |\uparrow\downarrow\downarrow\uparrow\rangle + |\uparrow\uparrow\downarrow\downarrow\rangle + \frac{1}{2}\left(-J + \sqrt{8 + J^2}\right)\left[|\downarrow\uparrow\downarrow\uparrow\rangle + |\uparrow\downarrow\uparrow\downarrow\rangle\right] \ . \tag{3.43}$$

The energy for this state is $-J - \sqrt{8 + J^2}$. Figure 3.4 displays the regions where each state dominates. Each type of ground state has a definite S^z eigenvalue, since $[S^z, H] = 0$. This eigenvalue is the magnon number, the number of down spins L_-, introduced previously. When the coupling is changed to spin-dot coupling, however, the patterns change. Now, the the ferromagnetic ordered state is the

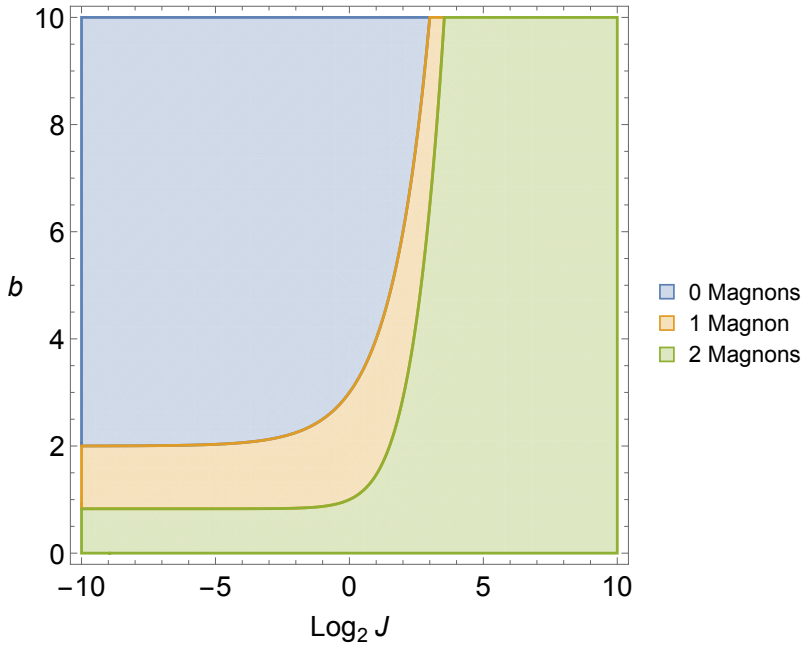

Figure 3.4: The values of b and J determine which eigenstate of the system has the least energy. They are characterized by magnon number, the number of down spins L_-.

ground state for all values of J and b. Additionally, the second-lowest energy state is the zero-momentum magnon state. Figure 3.5 shows the energy levels for this coupling, which differs only from above by the addition of a $S^z_{m_1} S^z_{m_2}$ term in the Hamiltonian. There are thirteen distinct energy levels, so the degeneracy here is lower than for the plus-minus coupling. As J increases, the energy levels asymptote to three distinct groups, which grow like $-J$ (9 states), J (6 states), and $3J$ (1 state).

For $L = 8$, the Hilbert space has 256 dimensions, so graphs like Fig. 3.3 will not be as instructive. However, the same steps were performed: generating the spin operators from tensor products, summing them together to form the Hamiltonian, diagonalizing, and inspecting the eigenstates. The energy states of the plus-minus coupling display a similar pattern to those for the smaller system, shown in Fig. 3.6. As J increases and b decreases, the magnon number of the ground state increases from 0 to 4.

For the spin-dot coupling, the story is again the same; the state with all spins up has the lowest energy for all parameter values. As we generalize to larger ensembles it will always be possible to pick parameter values such that the ground state is the simple, ordered one. This fact will be important in the introduction of thermal fluctuations and calculation of thermodynamic properties in Chapter 4.

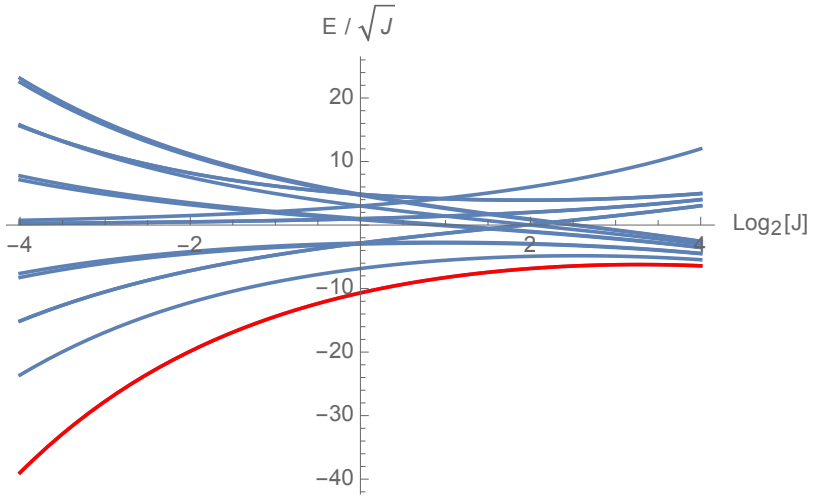

Figure 3.5: The energy levels of the $L = 4$ 2-adic system with spin-dot coupling. The magnetic field is set to $b = 4.22$ for this figure. The red line highlights the ground state $|\uparrow\uparrow\uparrow\uparrow\rangle$ which has the lowest energy regardless of b and J.

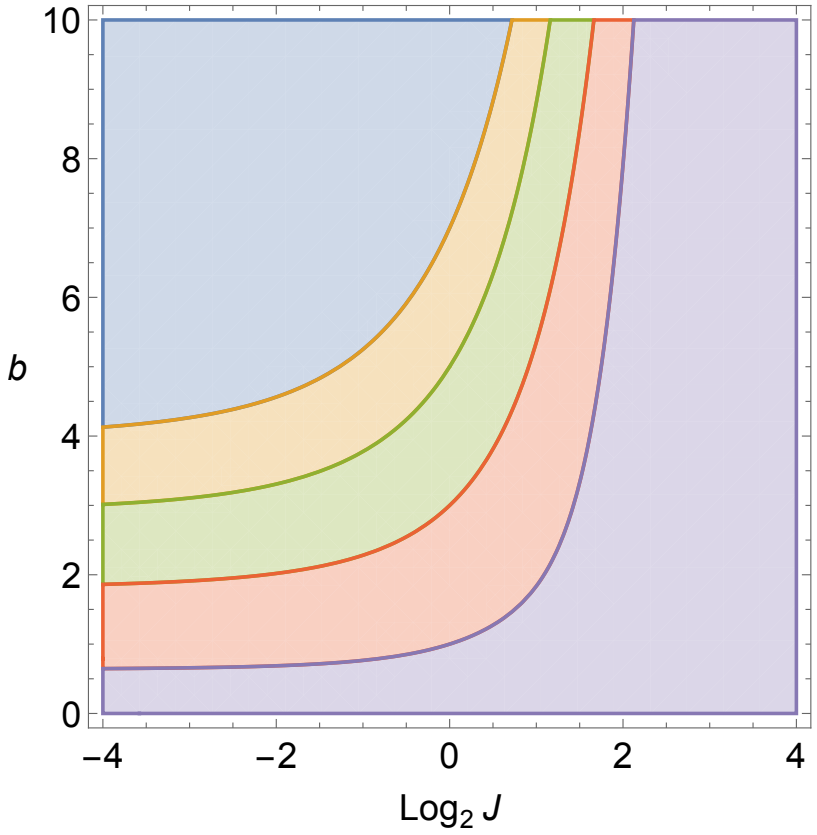

Figure 3.6: The regions of different ground states for $L = 8$. The magnon number begins at 0 in the blue corner and increases towards the bottom right purple region (4 magnons).

Chapter 4

Thermodynamic Limit

As the number of particles in the system increases, it becomes more and more difficult to calculate energies and eigenstates explicitly. Instead, we will make some assumptions about how the system behaves as $L \to \infty$ and make note of its macroscopic properties. In particular, we assume that low-energy thermal fluctuations of the system correspond to small collective oscillations around the ordered state. We have shown in Chapter 3 that it is possible to pick values of b and J such that the ordered state or the one magnon state have the least energy. In the case of spin-dot coupling, the ordered state always has the least energy and a one-magnon state has the next-lowest, regardless of b and J. These excitations are bosons: they have integer spin and obey Bose-Einstein statistics. It is possible to rigorously demonstrate the bosonic nature of the magnons using the Holstein-Primakoff representation of spin operators , but viewing them as lattice excitations provides some intuition. should I do this Vibrations, whether of physical particles or of spins, are additive; the addition of another quantum of energy just creates a larger vibration in the same mode. The additive nature is another way of stating that there can be several magnons with the same momentum k: magnons do not obey the Pauli exclusion principle.

4.1 Specific Heat: Heisenberg Model

We begin with a treatment of the standard Heisenberg model, using nearest neighbor coupling (3.18). The magnon dispersion relation $\omega \approx J_* k^2 a^2$ can be used to calculate the specific heat for the excitations of spin waves in the system. Specific heat is the derivative of the system's energy with respect to temperature. It is an experimentally accessible quantities, and its scaling with T in the limit of small T is a good first indicator of what kind of degrees of freedom are present at

low energies. As with phonons or photons, these undulatory excitations have the energy levels of a harmonic oscillator

$$E = \sum_k \hbar\omega_k \left(n_k + \frac{1}{2}\right) \tag{4.1}$$

where n_k denotes the number of magnons excited in the mode $\vec{k}$. To allow $\langle n_k \rangle > 1$ is a restatement of the fact that magnons are bosons. Using the assumption that most excitations are simple harmonic oscillations, a spin chain system in thermal equilibrium follows the Planck distribution, so

should I continue using $\hbar = k_B = 1$?

$$\langle n_k \rangle = \frac{1}{\exp(\hbar\omega_k/k_BT) - 1} \tag{4.2}$$

Using this occupation factor, the average energy can be calculated:

$$U = \langle E \rangle = \sum_k \hbar\omega_k \left(\langle n_k \rangle + \frac{1}{2}\right) = E_0 + \sum_k \frac{\hbar\omega_k}{\exp(\hbar\omega_k/k_BT) - 1}. \tag{4.3}$$

The specific heat follows immediately since $C_V = \frac{dU}{dT}$. The only remaining barrier is the calculation of the sum in (4.3), which is really an integral in $\vec{k}$ space:

$$\sum_{\vec{k}} \cdots = \frac{V}{(2\pi)^3} \int d^3\vec{k} \cdots \tag{4.4}$$

We will also use the low temperature limit: as $T \to 0$, only magnons with low values of $|k|$ will be excited, so we can approximate $\hbar\omega \approx J_* a^2 k^2$. This implies

$$U = E_0 + \frac{V}{(2\pi)^3} \int_0^\infty 4\pi k^2 \frac{J_* a^2 k^2}{\exp(J_* a^2 k^2/k_BT) - 1} dk. \tag{4.5}$$

With a change of variables $x = k\sqrt{J_* a^2/k_BT} = k\sqrt{D/k_BT}$, the integral simplifies to

$$E_0 + \frac{V}{2\pi^2} D^{-3/2} (k_BT)^{5/2} \int x^4 \frac{dx}{e^{x^2} - 1}. \tag{4.6}$$

The integral is now dimensionless and is easily calculated: it equals $\frac{3}{8}\sqrt{\pi}\zeta(\frac{5}{2})$. The important part is the temperature dependence $U \propto (k_BT)^{5/2}$ so we get

$$\boxed{C_V = \frac{dU}{dT} \propto \left(\frac{k_BT}{D}\right)^{3/2}}. \tag{4.7}$$

The exponent of 3/2 is the source of the name of this law: the Bloch $T^{3/2}$ law. The exponent is different for photons and phonons due to differences in dispersion relation.

4.2 Specific Heat: p-adic coupling

It is possible to adjust the dispersion relation in (4.5) to find the average energy and specific heat in a system with the p-adic coupling 3.37. In one dimension, the average energy still satisfies

$$\langle E \rangle = \int_{\mathbb{Q}_p} \frac{k^2}{e^{k^2/k_B T} - 1} dk. \tag{4.8}$$

The boson occupation factor of $(e^{\hbar\omega/k_B T} - 1)^{-1}$ remains the same, since the underlying mechanism of quantum harmonic oscillation remains the same. All that changes is the dispersion relation, so that $\omega \propto |k|_p^s$ for some $s > 0$. Using this replacement, the integral in (4.8) becomes

$$U = E_0 + \frac{1}{2} \int \frac{|k|_p^s}{\exp(|k|_p^s/T) - 1} dk. \tag{4.9}$$

with L a length and D some constant of proportionality. Although the derivation in 4.1 used three dimensions, the dimension of the p-adic space can be folded into the choice of parameter s, with some appropriate scaling of T in the argument of the exponential. Now the integral can be turned into a sum as in section 2.3:

$$U = \langle E \rangle = \frac{L}{2\pi} \sum_{n=-\infty}^{\infty} \frac{p^{-ns}}{\exp(p^{-ns}/T) - 1} (p^{-n}) \left(1 - \frac{1}{p}\right) \tag{4.10}$$

This is an ugly sum, but it does converge. For large positive values of n, the exponential can be Taylor expanded and the sum reduces to a geometric series; for large negative values of n, the exponential dominates and drives the terms quickly to zero. Because n ranges from positive to negative infinity, it is difficult to narrow down this integral into low-T or high-T limits.

Let us analyze the interesting part of the sum

$$S(T) = \sum_{n=-\infty}^{\infty} \frac{p^{-n(s+1)}}{exp\,(p^{-ns}/T) - 1} \tag{4.11}$$

in terms of the definition

$$T \equiv p^{-n_* s}. \tag{4.12}$$

The sum (4.11) can be written as

$$S(T) = \sum_{n=-\infty}^{\infty} \frac{p^{-n(s+1)}}{exp\left(p^{(n_*-n)s}\right)-1} = T^{1+\frac{1}{s}} \sum_{n=-\infty}^{\infty} \frac{p^{(n_*-n)(s+1)}}{exp\left(p^{(n_*-n)s}\right)-1} \equiv T^{1+\frac{1}{s}} F(n_*). \tag{4.13}$$

Shifting n_* by an integer does not change the sum:

$$F(n_*) = F(n_*+1) \tag{4.14}$$

It is therefore possible to expand the function as a Fourier series

$$F(n_*) = \sum_{l=0}^{\infty} A_l \cos(2\pi l n_*) + \sum_{l=1}^{\infty} B_l \sin(2\pi l n_*). \tag{4.15}$$

The Fourier coefficients are given by

$$A_l = (2-\delta_l) \int_0^1 dx F(x) \cos(2\pi l x) = (2-\delta_l) \int_0^1 dx \sum_{n=-\infty}^{\infty} \frac{p^{(x-n)(s+1)}}{exp\left(p^{(x-n)s}\right)-1} \cos(2\pi l x) \tag{4.16}$$

$$= (2-\delta_l) \int_{-\infty}^{\infty} dx \frac{p^{(x-n)(s+1)}}{exp\left(p^{(x-n)s}\right)-1} \cos(2\pi l x), \tag{4.17}$$

and

$$B_l = 2 \int_{-\infty}^{\infty} dx \frac{p^{(x-n)(s+1)}}{exp\left(p^{(x-n)s}\right)-1} \sin(2\pi l x). \tag{4.18}$$

Eliminating n_* in favor of the original T, we find that

$$S(T) = T^{1+\frac{1}{s}} \left[A_0 + A_1 \cos\left(2\pi \log_p(T)/s\right) + B_1 \sin\left(2\pi \log_p(T)/s\right) + \cdots\right]. \tag{4.19}$$

For a large range of parameter values, the higher harmonics are sub-dominant, as illustrated below.

To get a handle on the exact behavior of (4.11), the sum can be numerically calculated. Appendix A.2 contains the MATLAB program used to sum terms of this series. The program first sets a value of $s \in [0.1, 4]$. Then, for $1 < T < 1000$, the terms of the series with $|n| < 20$ are summed. Because of the rapid drop-off of the terms, numerical calculation of the value for high n yields `Inf`, so adding terms with large n are negligible. For instance, with $s = 2$, $T = 10$, the value of the summand at $n_* = -2$ is 1.246. At $n = \pm 20$, the summand drops to 4.76×10^{-6} and $4.01 \times 10^{-47,751,183,256}$. It is therefore a safe assumption to truncate the sum, except at very low values of s close to 0, when the terms are relevant up to $n = -150$. With $s \approx 0$, however, the coupling is essentially all-to-all with equal interaction energies ($J_h^{p-\text{adic}} \approx 1$ for all h) and does not represent a regime of

interest. To capture the effect of changing both s and T, the sum was also done taking the terms from $n_* - 15 < n < n_* + 15$. This method actually yielded more realistic results, since it avoids the non-physical drop-off around $s = 0.63$ shown in Fig 4.2. For a given value of s, the summand (**??**) has a power law dependence. Figure 4.1 depicts the fitted power law $y = ax^b$ with $a = 0.89$ and scaling exponent $b = 1.49$. The fit begins as an overestimate and becomes an underestimate around $T = 360$, indicating a greater convexity than the power law fit can indicate. Figure 4.2 shows the

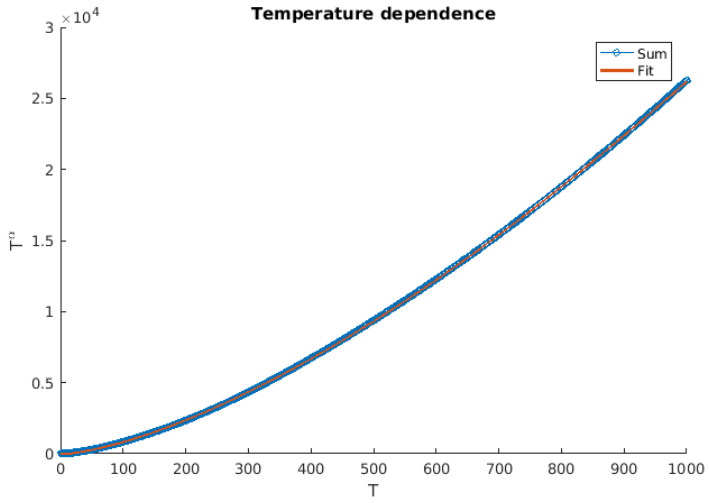

Figure 4.1: The dependence on temperature of the energy summand **??** for $s = 2$. The power law exponent α is 1.5.

behavior of the power law exponent α as a function of s. As mentioned above, the two different approximations of the sum yield similar results for $s \gtrsim 0.63$, below which the method of summing over a fixed range of n does not capture the rapidly changing behavior. Summing the significant terms in a window around n_*, by contrast, agrees remarkably well with the expected functional form $\alpha(s) = 1 + 1/s$. There is a small amount of sinusoidal variation in the sum which gets larger away from $s = 1$. Figure 4.3 demonstrates this phenomenon. Especially for smaller values of s, we may conclude that the average energy of the spin chain system with p-adic coupling behaves like

$$\langle E \rangle \sim T^{1+1/s} \tag{4.20}$$

and consequently the specific heat behaves like

$$C_V \sim T^{1/s}. \tag{4.21}$$

The greater the strength of non-local p-adic interactions, the lower the specific heat becomes for a

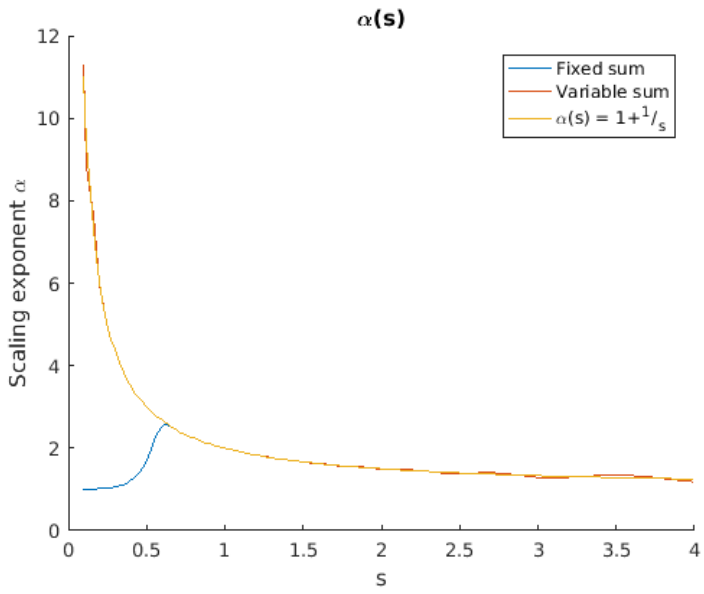

Figure 4.2: The temperature dependence of (4.11) takes a power law form. The exponent of the power law, α, depends on s as shown.

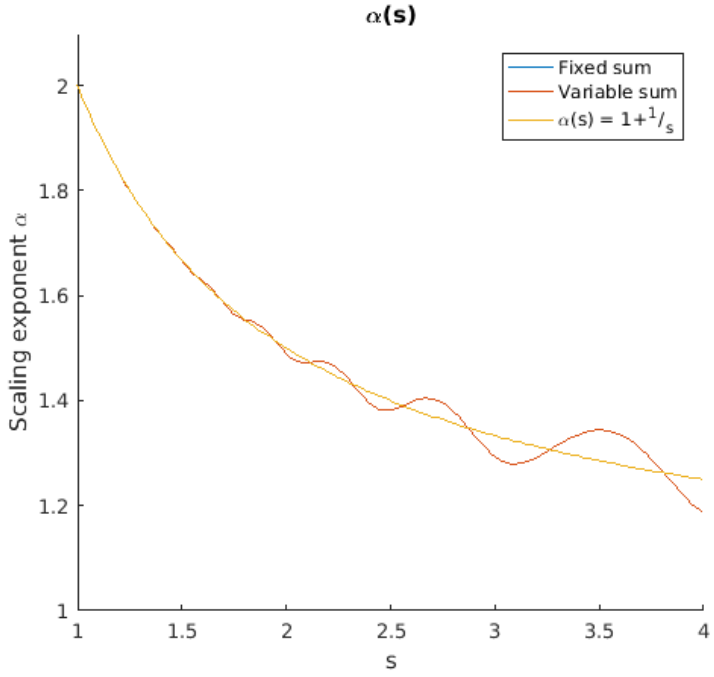

Figure 4.3: Sinusoidal behavior of scaling exponent α is more pronounced for large values of s.

given temperature, and the slower it grows as temperature increases. This effect may be due to a "decoupling" phenomenon: the system may separate into $L/2$ pairs of spins, with each site mainly interacting with the unique site p-adically closest to it.

4.3 Magnetization

The magnetization $\vec{M} = (1/L)\sum_m \langle S_m^z \rangle$ is a natural measure of the strength of the magnetic order in a system. If $|\vec{M}| = 0$, we say the system is disordered; if it is positive, there is a degree of order. $\vec{M}$ is an example of an order parameter, which indicate the boundaries between different phases of a system. The magnetization is related to the L_-, the number of down spins, by

$$M = \frac{1}{L}\sum_m \langle S_m^z \rangle = \frac{1}{2} - \frac{1}{L}\langle L_- \rangle = \frac{1}{2} - \sum_k \langle n_k \rangle \equiv \frac{1}{2} - \Delta M. \tag{4.22}$$

For the totally ordered state, $\Delta M = 0$ and the magnetization $M = \frac{1}{2}$. It is useful to look at how ΔM behaves at low temperatures, when our assumption of oscillations around the ordered state holds. First, we introduce an arbitrary lower bound for the wavevector, called k_0, which represents the lowest allowed momentum for a magnon. In reality, $k_0 = 0$. We also define another wavevector $\bar{k}$, such that for $|k| < \bar{k}$, the quadratic approximation 3.34 is valid. Then the magnetization can be written as

$$\Delta M = \frac{1}{L}\left(\sum_{k_0 < |k| < \bar{k}} \frac{1}{\exp\left(J_* a^2 k^2 / k_B T\right) - 1} + \sum_{|k| > \bar{k}} \frac{1}{\exp\left(\omega_k / k_B T\right) - 1} \right). \tag{4.23}$$

Because the second sum is independent of k_0 and is finite, we focus our attention on the first sum for the moment. Expanding the exponential as a Taylor series and converting to an integral, we find

$$\Delta M \propto \int_{k_0}^{\bar{k}} dk\ k^{d-1} \frac{k_B T}{J_* a^2 k^2} \propto \frac{k_B T}{J_* a^2} \cdot \begin{cases} 1/k_0 + \ldots, & d = 1 \\ -\log k_0 + \ldots, & d = 2 \end{cases} \tag{4.24}$$

where d is the dimension of the system. In either both cases, the magnetization ΔM diverges as $k_0 \to \infty$, indicating that the assumption of small $\langle L_- \rangle$ is invalid and that $M = 0$, i.e., there is no magnetic order in 1 or 2 dimensions.

again, this is in HP representation so maybe I should write it

For our p-adic system, a similar analysis can be performed.

Chapter 5

Conclusion

The main results of this thesis are the exploration of the quantum energy levels and thermodynamic properties of a spin chain system with p-adic interactions. The spin chain system plays the role of a CFT over the p-adic numbers $\mathbb{Q}_p$, a field which is the natural boundary of the Bruhat-Tits tree T_p. This connection between tree and boundary is a discrete version of the AdS/CFT correspondence. For a p-adic spin system, we take the well-studied nearest-neighbor interactions of the Heisenberg model (3.18) and replace them with a coupling whose strength depends on the p-adic distance between sites (3.37). The Hamiltonian for this all-to-all interaction still commutes with translation operator U and components of the total spin operator like S^z_{total}, so we expect energy states to have a wave-like form with definite z spin. For systems with $L = 4$ and $L = 8$, there are regions in the parameter space of coupling strength J and magnetic field b that allow the ground state to be either the ordered state or the zero-momentum magnon. In fact, when the spins interact through their dot product $\vec{S}_i \cdot \vec{S}_j$, the ordered state is always the lowest energy. We assume that when the number of sites grows large, excitations from the ground state are low-energy, non-interacting, diffuse magnons, and that the long-range interactions do not substantially increase the energy. With this simplification in mind, we use the magnon dispersion relation (3.34) to calculate the average energy and specific heat of magnons in thermal equilibrium. These quantities have power law behavior for low temperature: $\langle E \rangle \sim T^{1+1/s}$ and $C_V \sim T^{1/s}$, with minor sinusoidal variations given by a Fourier series (4.19). As the strength of the p-adic interaction increases, these quantities are less sensitive to temperature changes, heuristically due to a "decoupling" phenomenon.

Several generalizations to this work stand out as possible avenues for future progress. The first would be to generalize from the 2-adic numbers to higher values of p. To maintain a well-defined

notion of distance while keeping periodic boundary conditions, this adjustment would require the system size to be a power of 3. In a similar vein, the system could be constructed in higher dimensions. While we argued in section 4.2 that the dimensionality of the system was reflected in the size of the parameter s, the bulk of the Bruhat-Tits tree would have to change. Generalizing to $\mathrm{AdS}_{n+1}/\mathrm{CFT}_n$ would require the boundary to become the n-dimensional vector space $\mathbb{Q}_p^n$ and the bulk to be a tree with $p^n + 1$ neighbors for each vertex. There exist issues with defining an n-dimensional norm, which Gubser et. al. discuss in [6]. Explicit calculations of energy states and related quantities could add to the theoretical discussion. Finally, the AdS/CFT correspondence is developed in order to solve difficult problems in one theory with easier calculations in the other. Further research could look into what types of problems might require a holographic dictionary to convert the calculations, and what they would add to the connection between gravitation on the tree and quantum systems like the ones discussed here.

Appendix A

Code

A.1 Numerical Diagonalization

```
Initialization

Enter the number of sites and the type of coupling.

RadioButtonBar[Dynamic[sitenum], {4, 8}]
RadioButtonBar[Dynamic[coupling], {"SpinDot", "SpinXY"}]

OuterTimes[A_,
   B_] :=(*Outer product of two lists to give a matrix*)(CC =
    Table[0, {i, 1, Length[A] Length[B]}, {j, 1,
      Length[A[[1]]] Length[B[[1]]]}];
   Do[CC[[Length[B] (i - 1) + k, Length[B[[1]]] (j - 1) + l]] =
     A[[i, j]] B[[k, l]], {i, 1, Length[A]}, {j, 1, Length[A[[1]]]}, {k, 1,
     Length[B]}, {l, 1, Length[B[[1]]]}];
   CC);
OuterTimes[A_, B_, CC__] := OuterTimes[OuterTimes[A, B], CC];

\[Sigma]z = {{1, 0}, {0, -1}};
\[Sigma]y = {{0, -I}, {I, 0}};
\[Sigma]x = {{0, 1}, {1, 0}};
\[Delta] = IdentityMatrix[2];

SpinMatrix[i_, w_] := (
   sites = {\[Delta], \[Delta], \[Delta], \[Delta], \[Delta], \[Delta], \
\[Delta], \[Delta]};
   Which[w == "x", sites[[i]] = \[Sigma]x/2, w == "y",
    sites[[i]] = \[Sigma]y/2, w == "z", sites[[i]] = \[Sigma]z/2];
   If[sitenum == 8,
    Return[
     OuterTimes[sites[[1]], sites[[2]], sites[[3]], sites[[4]], sites[[5]],
      sites[[6]], sites[[7]], sites[[8]]]],
    Return[OuterTimes[sites[[1]], sites[[2]], sites[[3]], sites[[4]]]]]);
```

```
sx = Range[sitenum];
sy = Range[sitenum];
sz = Range[sitenum];

Do[sx[[i]] = SpinMatrix[i, "x"], {i, sitenum}]
Do[sy[[i]] = SpinMatrix[i, "y"], {i, sitenum}]
Do[sz[[i]] = SpinMatrix[i, "z"], {i, sitenum}]

SpinDot[i_, j_] :=
  SparseArray[(sx[[i]].sx[[j]]) + (sy[[i]].sy[[j]]) + (sz[[i]].sz[[j]])];
SpinXY[i_, j_] := SparseArray[(sx[[i]].sx[[j]]) + (sy[[i]].sy[[j]])];

SzTotal = Sum[sz[[i]], {i, 1, sitenum}];

spinvec = StringJoin /@ Tuples[{"u", "d"}, sitenum];

H = 2 Switch[{sitenum, coupling},
    {4, "SpinDot"},
    Normal[-J (SpinDot[1, 2] + SpinDot[2, 3] + SpinDot[3, 4] +
          SpinDot[4, 1]) - J (SpinDot[1, 3] + SpinDot[2, 4])] -
     b /2 Sum[sz[[i]], {i, 1, sitenum}],
    {4, "SpinXY"},
    Normal[-J (SpinXY[1, 2] + SpinXY[2, 3] + SpinXY[3, 4] + SpinXY[4, 1]) -
       J (SpinXY[1, 3] + SpinXY[2, 4])] - b /2 Sum[sz[[i]], {i, 1, sitenum}],
    {8, "SpinDot"}, -(Sum[SpinDot[i, Mod[i + 1, 8, 1]], {i, 1, 8}] +
        Sum[SpinDot[i, Mod[i + 3, 8, 1]], {i, 1, 8}]) -
     J (Sum[SpinDot[i, Mod[i + 2, 8, 1]], {i, 1, 8}]) -
     J^2 (Sum[SpinDot[i, Mod[i + 4, 8, 1]], {i, 1, 4}]) -
     SparseArray[b/2 Sum[sz[[i]], {i, 1, sitenum}]],
    {8, "SpinXY"}, -(Sum[SpinXY[i, Mod[i + 1, 8, 1]], {i, 1, 8}] +
        Sum[SpinXY[i, Mod[i + 3, 8, 1]], {i, 1, 8}]) -
     J (Sum[SpinXY[i, Mod[i + 2, 8, 1]], {i, 1, 8}]) -
     J^2 (Sum[SpinXY[i, Mod[i + 4, 8, 1]], {i, 1, 4}]) -
     SparseArray[b /2 Sum[sz[[i]], {i, 1, sitenum}]]];
```

A.2 Specific Heat Sum

```
%For the p-adic specific heat integral, this script calculates and plots
%the temperature scaling exponent alpha as a function of s.

p=2;                              %p-adic base
s=linspace(0.1,4,200);            %s vector
alpha = zeros(2,length(s));       %alpha vector
temp = linspace(0.001,1,1000);    %temperature vector

for i=1:length(s)
    sumfixed=zeros(1,1000);       %calculate the sum two ways
    sumvar  =zeros(1,1000);
    for j = 1:length(temp)
```

```
        nstar = round(-log(temp(j))/s(i)/log(p));   %significant n value

        %sum from n = -20 to n = 20
        for n = -20:20
            summand = (1-1/p)*p^(-n)*p^(-n*s(i))/(exp(p^(-n*s(i))/temp(j))-1);
            if(isinf(summand) || isnan(summand))
                summand = 0; %replace Inf or NaN values
            end
            sumfixed(j) = sumfixed(j) + summand;
        end

        %sum 15 terms around nstar
        for n = (nstar-15):(nstar+15)
            summand = (1-1/p)*p^(-n)*p^(-n*s(i))/(exp(p^(-n*s(i))/temp(j))-1);
            if(isinf(summand) || isnan(summand))
                summand = 0; %replace Inf or NaN values
            end
            sumvar(j) = sumvar(j) + summand;

        end
    end

    %fit power law plot to p-adic integral vs. temperature
    valsfixed = coeffvalues(fit(temp',sumfixed','power1'));
    valsvar = coeffvalues(fit(temp',sumvar','power1'));
    alpha(1,i) = valsfixed(2);
    alpha(2,i) = valsvar(2);
end

figure
hold on;

plot(s,alpha(1,:))
plot(s,alpha(2,:))
plot(s,1+(1./s))    %expected form is (1+s)/s

legend('Fixed sum','Variable sum','\alpha(s) = 1+^1/_s')
xlabel('s')
ylabel('Scaling exponent \alpha')
title('\alpha(s)')
```

Bibliography

[1] Kip S. Thorne Charles W. Misner and John Archibald Wheeler. *Gravitation*. New York: W. H. Freeman and Company, 1970.

[2] J. Maldacena. "The Large-N Limit of Superconformal Field Theories and Supergravity". In: *International Journal of Theoretical Physics* 38 (1999), pp. 1113–1133. DOI: 10.1023/A:1026654312961. eprint: hep-th/9711200.

[3] S. S. Gubser, Igor R. Klebanov, and Alexander M. Polyakov. "Gauge theory correlators from noncritical string theory". In: *Phys. Lett.* B428 (1998), pp. 105–114. DOI: 10.1016/S0370-2693(98)00377-3. arXiv: hep-th/9802109 [hep-th].

[4] Edward Witten. "Anti-de Sitter space and holography". In: *Adv. Theor. Math. Phys.* 2 (1998), pp. 253–291. DOI: 10.4310/ATMP.1998.v2.n2.a2. arXiv: hep-th/9802150 [hep-th].

[5] Juan Maldacena. "The Illusion of Gravity". In: *Scientific American* (293), pp. 56–63. URL: http://www.sns.ias.edu/~malda/sciam-maldacena-3a.pdf.

[6] Steven S. Gubser et al. "p-adic AdS/CFT". In: *Commun. Math. Phys.* 352.3 (2017), pp. 1019–1059. DOI: 10.1007/s00220-016-2813-6. arXiv: 1605.01061 [hep-th].

[7] Daniel Gift. "Gravity on the Bruhat-Tits Tree". Unpublished. Princeton, NJ: Princeton University.

[8] L. Brekke and P. G. O. Freund. "p-adic numbers in physics". In: *Phys. Rept.* 233 (1993), pp. 1–66. DOI: 10.1016/0370-1573(93)90043-D.

[9] Mihnea Popa. *Modern aspects of the cohomological study of varieties*. 2011. URL: http://www.math.northwestern.edu/~mpopa/571/chapter3.pdf.

[10] Steven Gubser. *unpublished notes*. 2017.

[11] Carsten Timm. *Theory of Magnetism. International Max Planck Research School for Dynamical Processes in Atoms, Molecules and Solids*. Technische Universitat Dresden, Institute for Theoretical Physics. URL: https://www.physik.tu-dresden.de/~timm/personal/teaching/thmagw09/lecturenotes.pdf.

[12] Edward B. Burger. *A Mathematical Seduction*. Mathematical Association of America. Feb. 2002. URL: https://web.williams.edu/Mathematics/eburger/BurgerMathHorizons.pdf.

[13] Charles Kittel. *Elementary solid state physics; a short course*. New York: Wiley, 1962.

[14] Enrico Rastelli. *Statistical Mechanics of Magnetic Excitations. From Spin Waves to Stripes and Checkerboards*. Series on Advances in Statistical Mechanics 18. Singapore: World Scientific Publishing Co. Pte. Ltd., 2013.

[15] Daniel D. Stancil and Anil Prabhakar. *Spin Waves. Theory and Applications*. New York: Springer, 2009.

[16] B. Dragovich et al. "On p-Adic Mathematical Physics". In: *Anal. Appl.* 1 (2009), pp. 1–17. arXiv: 0904.4205 [math-ph].

[17] Andrew Baker. *An Introduction to p-adic Numbers and p-adic Analysis*. School of Mathematics & Statistics, University of Glasgow. Nov. 2017. URL: http://www.maths.gla.ac.uk/~ajb/dvi-ps/padicnotes.pdf.

[18] Steven S. Gubser. "A p-adic version of AdS/CFT". In: (2017). arXiv: 1705.00373 [hep-th].

[19] Christopher Jagoe. "Chaotic Interactions in Anti-de Sitter Space". unpublished. Princeton University, Jan. 2017.

[20] Ezer Melzer. "NONARCHIMEDEAN CONFORMAL FIELD THEORIES". In: *Int. J. Mod. Phys.* A4 (1989), p. 4877. DOI: 10.1142/S0217751X89002065.

[21] Charlotte Mason Joseph Conlon and Edward Hughes. *Why String Theory?* University of Oxford. 2012. URL: http://whystringtheory.com/.